



DØ note 4751-CONF

Measurement of the Inclusive Jet Cross Section in $p\bar{p}$ Collisions at $\sqrt{s} = 1.96$ TeV

The DØ Collaboration
URL: <http://www-d0.fnal.gov>

(Dated: March 11, 2005)

We present a new preliminary measurement of the inclusive jet cross section in $p\bar{p}$ collisions based on an integrated luminosity of 378 pb^{-1} . The data were acquired using the DØ detector between 2002 and 2004. Jets are reconstructed using an iterative cone algorithm with radius $R_{\text{cone}} = 0.7$. The inclusive jet cross section is presented as a function of transverse jet momentum in two rapidity regions between 0.0 and 0.8. Predictions from next-to-leading order perturbative QCD calculations are in good agreement with the measured cross section.

Preliminary Results for Winter 2005 Conferences

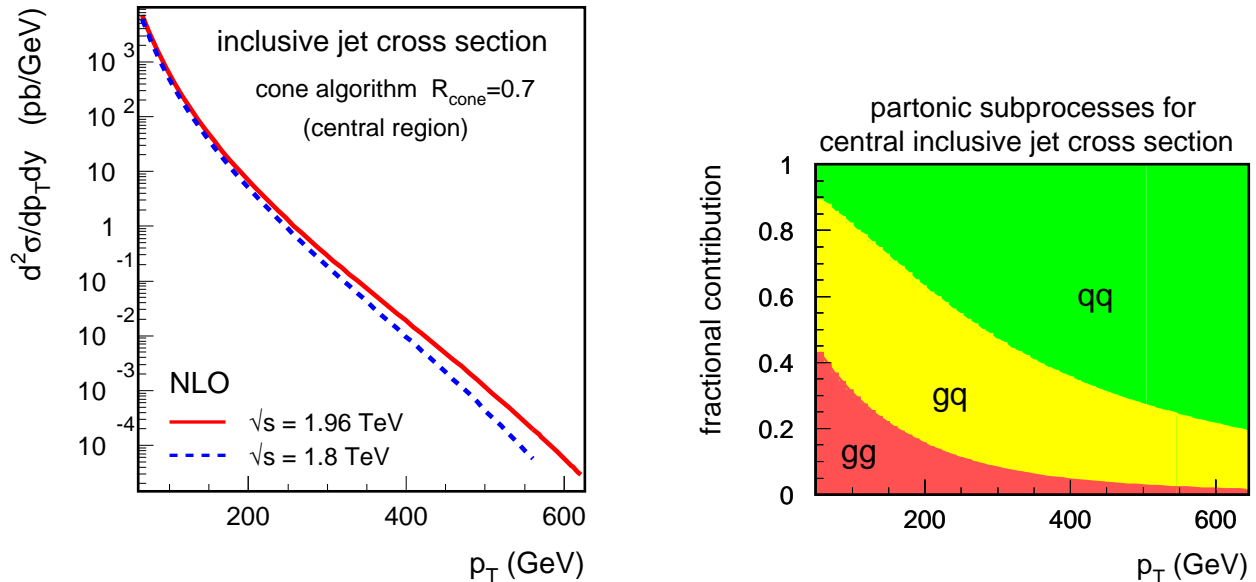


FIG. 1: The NLO pQCD predictions for the central inclusive jet cross section in $p\bar{p}$ collisions at two different center-of-mass energies (left) and the fractional contributions from different partonic subprocesses for $\sqrt{s} = 1.96$ TeV (right). The NLO predictions are made using CTEQ6.1M PDFs.

In the current Standard Model of particle physics, the production of particle jets in hadron collisions is described by the theory of Quantum Chromodynamics (QCD). When the transverse jet momentum with respect to the hadron beam direction (p_T) is large, the contributions from long-distance physics processes with low p_T can be neglected and the production rates of jets can be predicted by perturbative QCD (pQCD). The inclusive jet cross section in $p\bar{p}$ collisions at large p_T is directly sensitive to the strong coupling constant (α_s) and the parton density functions (PDFs) of the proton. Deviations from the pQCD prediction at high p_T , not explained by PDFs or α_s , may indicate new physics beyond the Standard Model. In Run II of the Fermilab Tevatron Collider the center-of-mass energy was increased to $\sqrt{s} = 1.96$ TeV, as compared to $\sqrt{s} = 1.8$ TeV in Run I. Even this moderate increase in the center-of-mass energy leads to a significant increase in the inclusive jet cross section at high p_T . At $p_T = 500$ GeV the cross section increases by almost 300% according to the pQCD prediction as shown in Figure 1 (left). Together with the increased integrated luminosity in Run II this extends the accessible p_T range and allows us to test pQCD at previously unexplored energies. The fractional contributions to the inclusive jet cross section from different partonic subprocess are displayed in Fig. 1 (right). It is seen that at low p_T the jet cross section is dominated by gluon-gluon and gluon-quark induced processes, while at high p_T quark-quark scattering gives the dominant contribution. At $p_T = 500$ GeV, however, there is still a contribution of $\approx 30\%$ from gluon-quark scattering, and thus some sensitivity to the gluon density in the proton which is here probed at large momentum fractions $x \approx 0.3$.

In this note we present an updated preliminary measurement of the inclusive jet cross section at $\sqrt{s} = 1.96$ TeV, based on a data sample corresponding to an integrated luminosity of $L = 378 \text{ pb}^{-1}$. Data were acquired with the upgraded DØ detector [?] between 2002 and 2004 in Run II of the Fermilab Tevatron. Events used in this analysis were triggered by single jet triggers, based on energy deposited in calorimeter towers. Data selection was based on run quality, event properties, and jet quality criteria.

Jets are defined by the ‘‘Run II cone algorithm’’ [2] which combines particles within a circle of radius $R_{\text{cone}} = 0.7$ in rapidity (y) and azimuth (ϕ) around the cone axis using the ‘‘ E -scheme’’ (adding the particle four-vectors). ‘‘Particles’’ is here used as a generic term for calorimeter towers in the experiment, stable particles in a Monte Carlo event generator, or partons in a pQCD calculation. The direction of every particle serves as a seed which is used as the cone axis for a new proto-jet. The particles inside the cone radius around the axis are combined into a jet and the procedure is iterated until the jet axis coincides with the cone axis. Only non-identical solutions are kept. The algorithm is re-run using the midpoints between pairs of jets as additional seeds (this makes the procedure infrared safe). Jets with overlapping cones are merged if the overlap area contains more than 50% of the p_T from the lower p_T jet, otherwise the particles in the overlap region are assigned to the nearest jet.

The inclusive jet cross section is measured in two rapidity regions $|y| < 0.4$ and $0.4 < |y| < 0.8$. Data are corrected for the jet energy measurement, selection efficiencies, and for migrations due to p_T resolution. This correction procedure follows closely the one used in a previous measurement of the azimuthal decorrelation of jets in dijet production [4].

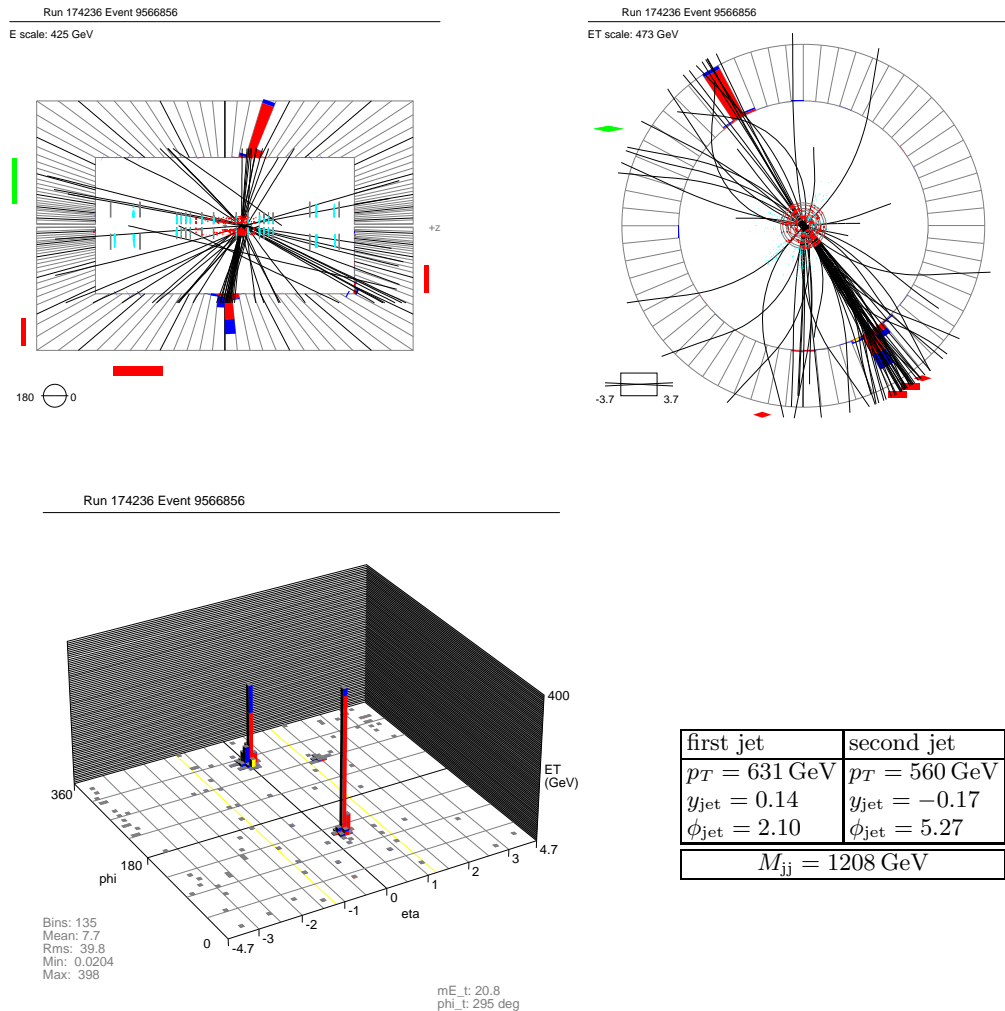


FIG. 2: Different views of the event that contains the jet with the highest transverse momentum in the data sample: side view parallel to the beam axis (top left), radial view (top right), and the calorimeter energy depositions in a lego plot in pseudo-rapidity and azimuthal angle (bottom).

The jet energy calibration was determined from the p_T imbalance in photon + jet events [3]. After the jet energy calibration is applied, spectra in p_T are fit, in an iterative procedure, with parameterized ansatz functions and smeared with resolutions determined from data. Ratios of the original to the smeared ansatz functions are used to correct the data for migration effects. The event with the highest p_T jet in the data sample is shown in Fig. 2. Detailed information is given in the table in Fig. 2. The leading jet has $p_T = 631 \text{ GeV}$ and is balanced in p_T by a second jet which is opposite in azimuthal angle. The invariant mass of the dijet system is $M_{\text{jj}} = 1208 \text{ GeV}$ which is 60% of the available proton-antiproton center-of-mass energy. In pQCD such events are described by the scattering of two partons which both carry fractions of $x \approx 0.6$ of the proton's momenta.

The contributions from different triggers to the partially corrected jet p_T spectra are shown in Fig. 3 (no corrections for migrations due to resolution are applied at this stage). Once the jet p_T reaches the trigger turn-on point, the spectrum follows the p_T spectra of the triggers with lower p_T thresholds. While this demonstrates the relative efficiencies of the different jet triggers with respect to each other, the absolute trigger efficiency has been confirmed using a muon reference trigger. The dominant uncertainty in the cross section measurement is due to the jet energy calibration. Fig. 4 shows the relative variation of the jet cross section when the energy calibration is varied by one standard deviation in both directions. The uncertainties are largest at high p_T and are highly correlated between all bins. Further sources of uncertainty are due to the data selection efficiency, the trigger efficiency, the correction for migrations and the jet p_T resolution. In addition, the luminosity measurement has an uncertainty of 6.5%.

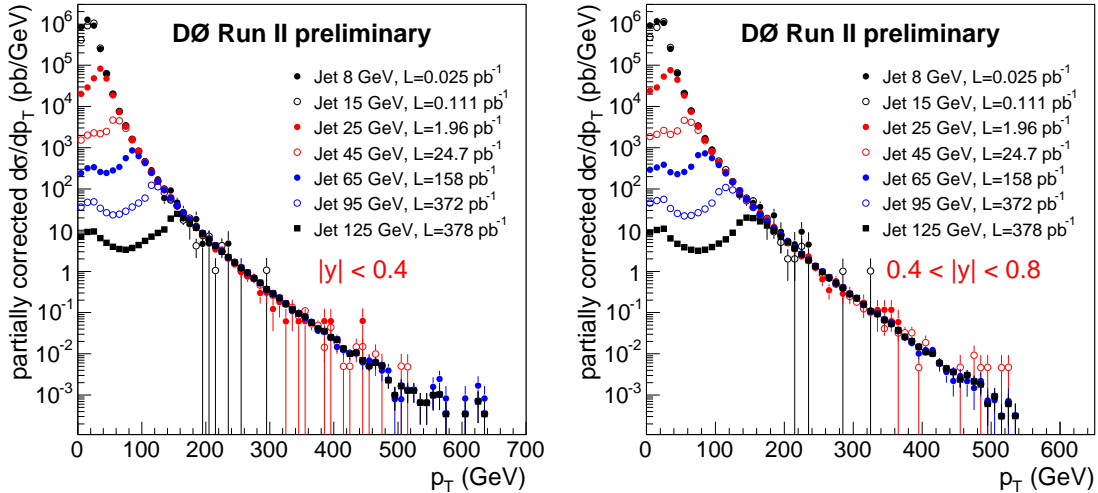


FIG. 3: The inclusive jet cross section in two rapidity ranges, measured with different jet triggers at different p_T thresholds. The trigger names in the legend include the nominal thresholds in GeV. Also quoted is the integrated luminosity for each trigger.

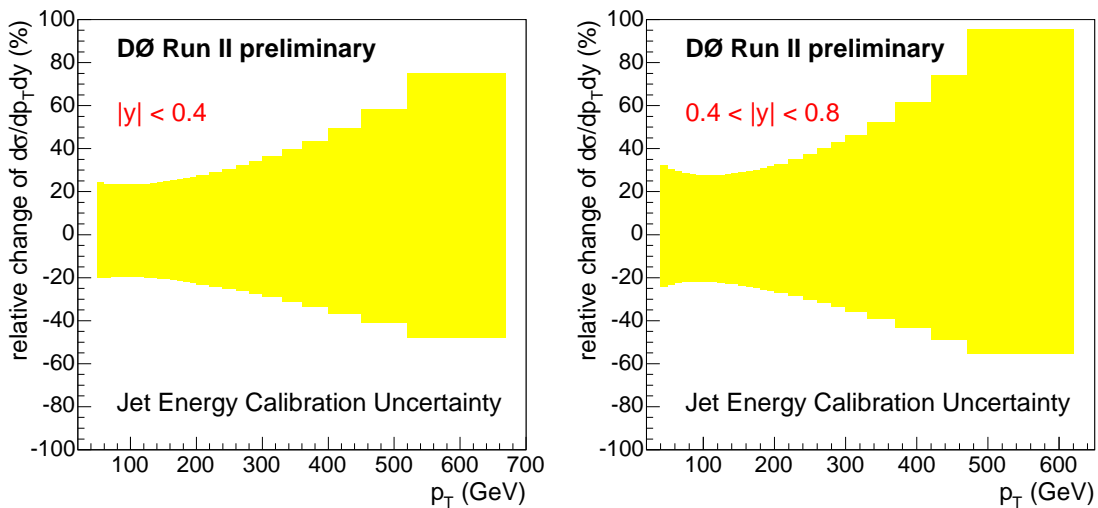


FIG. 4: The relative uncertainty of the inclusive jet cross section due to the uncertainty of the jet energy calibration in two rapidity ranges.

Predictions of next-to-leading (NLO) pQCD are computed using the program NLOJET++ [5] and the PDFs from CTEQ6.1M [6] and MRST2004 [7]. The renormalization and factorization scales are set to the transverse momenta of the individual jets $\mu_r = \mu_f = p_T$. A variation in scale by a factor of two is considered to be a part of the theoretical uncertainty. The Run II cone algorithm used in this analysis is infrared safe, allowing us to use exactly the same algorithm in the calculation that is used in the experimental measurement [8]. This avoids the ambiguities present in the Run I measurements where the jet definition was not infrared safe and an R_{sep} parameter was introduced in the theory calculation which was not matched to the experimental algorithm.

The contributions from soft (“non-perturbative”) processes to the jet cross section are studied in Fig. 5 using the PYTHIA [9] model. We investigate the relative effects from hadronization (solid line) and underlying event (dashed line) as a function of p_T in both rapidity regions. Hadronization corrections are here defined as the ratio of the jet cross section after and before hadronization. The correction due to the underlying event is defined as the ratio of

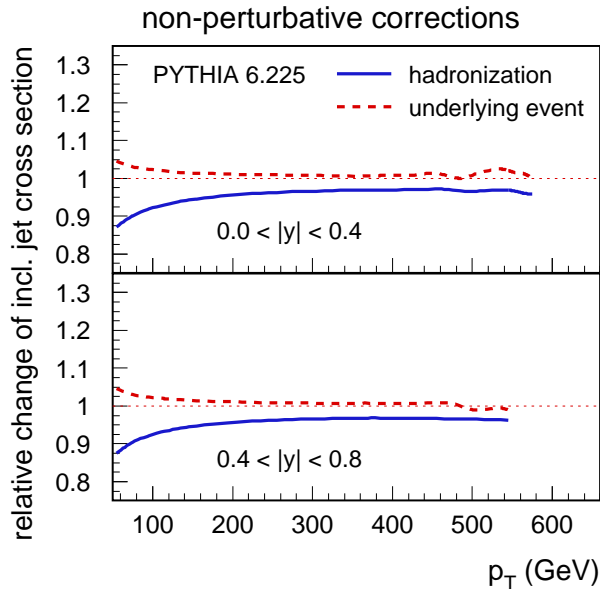


FIG. 5: The size of non-perturbative corrections for the inclusive jet cross sections is displayed as estimated by PYTHIA. The relative changes of the cross section due to hadronization (line) and underlying event (dashed line) are shown as a function of p_T in two rapidity regions.

the jet cross section with and without the underlying event simulation included. It is seen that both effects have opposite directions and are both below 5% for $p_T > 150$ GeV. The study has been redone using the HERWIG [10] model and the results are consistent with the PYTHIA results. A direct comparison of perturbative QCD calculations and experimental data is therefore meaningful within an uncertainty between 10% (below $p_T = 100$ GeV) and 5% (for $p_T > 100$ GeV).

The preliminary results of the measurement are shown in Fig. 6 as a function of p_T in two regions of rapidity with their full experimental uncertainty. The data at $|y| < 0.4$ are scaled up by a factor of ten for presentation purposes. In the range $50 < p_T < 670$ GeV the central jet cross section falls by eight orders of magnitude. The jet cross section at larger rapidity falls slightly more steeply towards high p_T than in the central region.

In Fig. 6 the predictions from NLO pQCD are overlaid on the data while the ratio of data and theory is shown in Fig. 7. The total experimental uncertainties are displayed as a band; the uncertainty of the NLO pQCD prediction due to the choice of the renormalization and factorization scales is displayed by the dashed and dotted lines. The uncertainties of the NLO prediction due to the PDF uncertainties have been determined using the 40 PDF sets from CTEQ6.1 [6], corresponding to up and down variations of the 20 eigenvectors which represent the uncertainties in the CTEQ PDF fit. The resulting uncertainties are indicated in Fig. 8 by the dashed lines; they show a strong increase with p_T , especially at larger rapidities. The NLO results for MRST2004 PDFs are shown as the dotted line in Fig. 8. The theoretical predictions describe the data within the experimental uncertainty over the whole p_T range in both rapidity regions. The experimental uncertainties are still too large to constrain the proton PDFs beyond their present precision.

Acknowledgments

We thank the staffs at Fermilab and collaborating institutions, and acknowledge support from the Department of Energy and National Science Foundation (USA), Commissariat à l’Energie Atomique and CNRS/Institut National de Physique Nucléaire et de Physique des Particules (France), Ministry for Science and Technology and Ministry for Atomic Energy (Russia), CAPES, CNPq and FAPERJ (Brazil), Departments of Atomic Energy and Science and Education (India), Colciencias (Colombia), CONACyT (Mexico), Ministry of Education and KOSEF (Korea), CONICET and UBACyT (Argentina), The Foundation for Fundamental Research on Matter (The Netherlands), PPARC (United Kingdom), Ministry of Education (Czech Republic), Natural Sciences and Engineering Research Council and West-Grid Project (Canada), BMBF (Germany), A.P. Sloan Foundation, Civilian Research and Development Foundation, Research Corporation, Texas Advanced Research Program, and the Alexander von Humboldt Foundation.

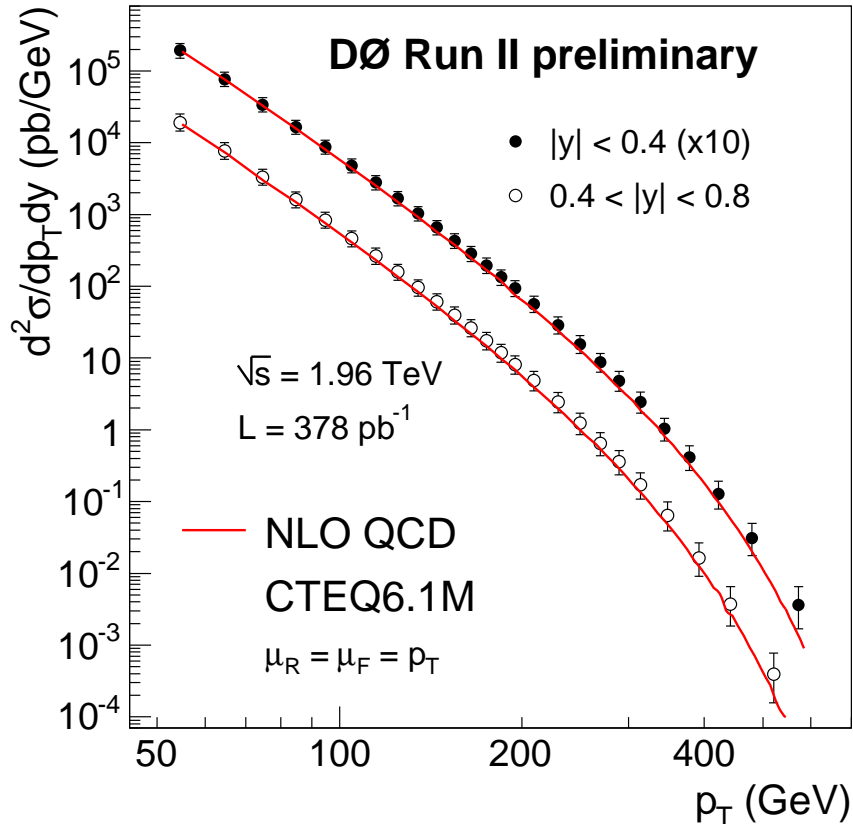


FIG. 6: The inclusive jet cross section, measured in two regions of jet rapidity. The error bars indicate the total experimental uncertainty. The data at $|y| < 0.4$ are scaled by a factor of ten for presentation purposes. The predictions from NLO pQCD are overlaid on the data.

-
- [1] V. Abazov *et al.* (DØ Collaboration), in preparation for submission to Nucl. Instrum. Methods Phys. Res. A; T. LeCompte and H. T. Diehl, Ann. Rev. Nucl. Part. Sci. **50**, 71 (2000); S. Abachi *et al.* (DØ Collaboration), Nucl. Instrum. Methods Phys. Res. A **338**, 185 (1994).
- [2] G. C. Blazey *et al.*, in *Proceedings of the Workshop: "QCD and Weak Boson Physics in Run II"*, edited by U. Baur, R. K. Ellis, and D. Zeppenfeld, Batavia, Illinois (2000) p. 47. See Section 3.5 for details.
- [3] B. Abbott *et al.* (DØ Collaboration), Nucl. Inst. and Meth. A **424**, 352 (1999).
- [4] V. Abazov *et al.* (DØ Collaboration), submitted to Phys. Rev. Lett., [hep-ex/0409040](#).
- [5] Z. Nagy, Phys. Rev. Lett. **88**, 122003 (2002); Z. Nagy, Phys. Rev. D **68**, 094002 (2003).
- [6] J. Pumplin *et al.*, JHEP **0207**, 12 (2002); D. Stump *et al.*, JHEP **0310**, 046 (2003).
- [7] A.D. Martin *et al.*, Phys. Lett. B **604**, 61 (2004)
- [8] M. H. Seymour, Nucl. Phys. B **513** (1998) 269. .
- [9] T. Sjöstrand *et al.*, Comp. Phys. Comm. **135**, 238 (2001).
- [10] G. Marchesini *et al.*, Comp. Phys. Comm. **67**, 465 (1992); G. Corcella *et al.*, JHEP **0101**, 010 (2001).

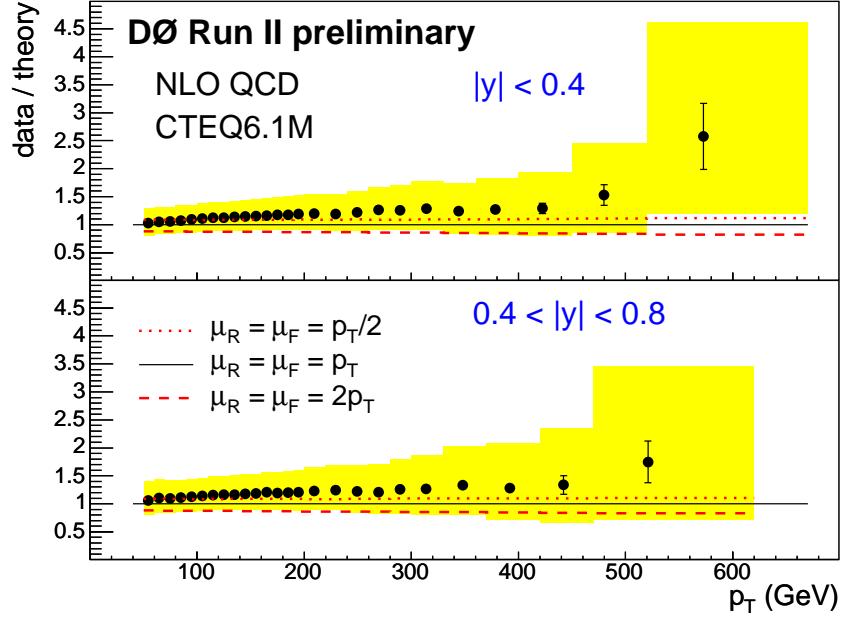


FIG. 7: The ratio of the measured inclusive jet cross section and the NLO pQCD prediction in two regions of jet rapidity. The total experimental uncertainty is shown by the shaded band. The scale dependence of the NLO calculation is indicated by the dashed and dotted lines.

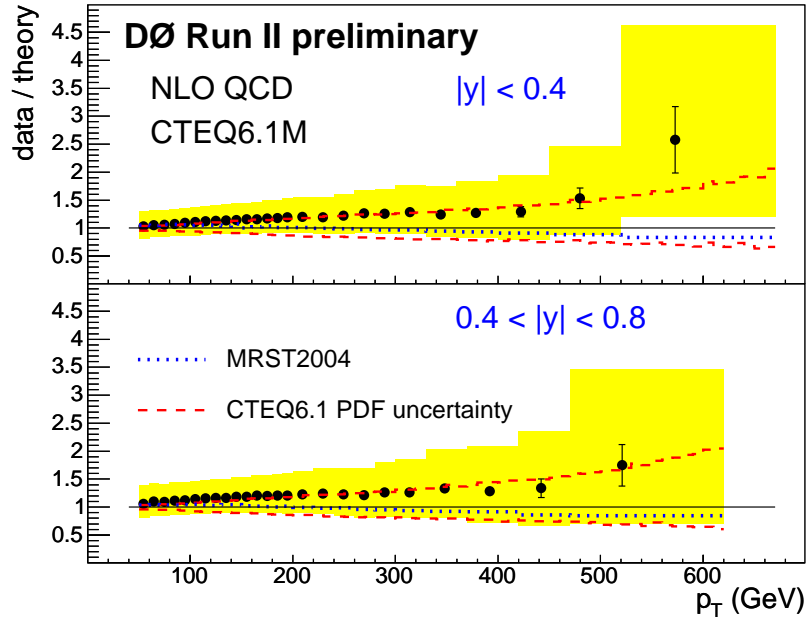


FIG. 8: The ratio of the measured inclusive jet cross section and the NLO pQCD prediction in two regions of jet rapidity. The total experimental uncertainty is shown by the shaded band. The uncertainty due to the proton PDFs is indicated by the dashed lines. The NLO prediction for MRST2004 PDFs are shown as the dotted line.